*Int. J. Electrochem. Sci.*, 14 **(2019)** 9007 – 9016, doi: 10.20964/2019.09.73

International Journal of
ELECTROCHEMICAL
SCIENCE
www.electrochemsci.org

# Influence of Al and Mn on the electrochemical performance of $LiNi_xCo_yM_{1-x-y}O_2$ as a cathode for Lithium-Ion Batteries

*Kai Yang, Min Zeng*[*], *Xin Wu, Yuqing Zhang, Yuan Bai*

School of Materials Science and Engineering, Southwest University of Science and Technology, Mianyang 621010, P R China
[*]E-mail: zengmin@swust.edu.cn

*Received:* 9 May 2019 / *Accepted:* 15 July 2019 / *Published:* 5 August 2019

Ternary cathode materials possess splendid application prospects in lithium-ion batteries. In this paper, cathode materials of $LiNi_{0.8}Co_{0.1}Mn_{0.1}O_2$ (811), $LiNi_{0.8}Co_{0.1}Mn_{0.05}Al_{0.05}O_2$ (811-Al) and $LiNi_{0.8}Co_{0.15}Al_{0.05}O_2$ (NCA) were prepared by a simple coprecipitation reaction. At the same time, to further explore how to improve the performance of the nickel-rich material, different elements and non-proportional substitutions were used to observe the charge/discharge performance of the battery. The 811 materials were found to have a capacity of 163 $mAhg^{-1}$ and, after 100 cycles at a rate of 0.1℃, maintained a capacity of 135 $mAhg^{-1}$, which represented a capacity retention of 82.7 %. On the other hand, the Al-substitution 811 materials were found to have low cycle performance and poor rate performance. These results indicate that Al and Mn in ternary materials have great differences in stabilizing the structure and properties of materials. As a result, the high-energy, high-density lithium-ion battery has great development potential at present.

**Keywords:** Cathode material, $LiNi_{0.8}Co_{0.1}Mn_{0.1}O_2$, NCA, Lithium-ion battery

## 1. INTRODUCTION

The lithium-ion battery plays an increasingly important role in life, and it is considered to be one of the most promising large-scale energy storage systems for hybrid electric vehicles and electric vehicles [1-3] and has the characteristics of long service life, high energy density, and high capacity [3]. However, the existing lithium-ion batteries also have many shortcomings, such as (i) high cost, mainly due to the cost of cathode materials, and (ii) poor cycle and rate performance. Therefore, only the development of lithium-ion batteries with high energy density can meet the needs of large-scale renewable energy [4]. In recent years, new materials, such as Li-Ni-Co-$MnO_3$ and Li-Ni-Co-$AlO_3$ ternary cathode materials have come to the fore. They have higher capacity, better safety, lower cost

and longer life than other types of batteries. At the same time, layered $LiNi_{0.8}Co_{0.1}Mn_{0.1}O_2$ (811) and $LiNi_{0.8}Co_{0.15}Al_{0.05}O_2$ (NCA) were considered to be two of the most promising cathode materials because of their wide application prospects [5-23]. Although $LiNi_xCo_yMn_{1-x-y}O_2$ provides attractive functions, further improvements and optimizations are needed in long-term cycling and thermal runaway due to its chemical composition [6-7]. The partial cation substitution (Al [8]) of Ni or Mn is a promising method to improve the capacity and rate capacity as well as the capacity retention [3]. In this experiment, Mn and Al were used as substitute elements to explore the effect of different stoichiometric ratios of elements on the performance of batteries. The results show that the substitution of Al will exacerbate the mixing of Li-Ni, but the substitution of Mn can inhibit this phenomenon. An electrochemical test shows that 811 have a characteristically high capacity, but the stability will decline.

At present, the preparation of ternary materials mainly includes high-temperature solid phase methods, coprecipitation methods, sol-gel methods, and spray drying methods. The morphology and structure of the materials synthesized by different methods are different, which affect their electrochemical properties. For example, the sol-gel method can make raw materials reach nanoscale mixing, whereas particles with high sphericity can be obtained by the coprecipitation method. In this experiment, ternary 811 and NCA cathode materials were prepared by co-precipitation. The nickel-drilling manganese ternary material prepared by the co-precipitation method can be mixed at the molecular or atomic level, which can solve the problems of unevenness and excessive particle size in the traditional solid-phase mixing process. The nickel-drilled manganese ternary material has a high purity, small particle size, uniform distribution and good sintering performance.

## 2. EXPERIMENT

### *2.1 Materials synthesis:*

First, $NiSO_4·6H_2O$, $CoSO_4·7H_2O$ and $MnSO_4·H_2O$ (the molar ratio was 8:1:1) particles were measured and dissolved in distilled water to prepare a mixed salt solution [9]. Because of the volatile effect of alcohol, the mixed salt solution was prepared by adding a small amount of alcohol at the same time as the salts. The water in the mixed salt can be absorbed, so the concentration of the mixed salt can be increased in phase. Second, according to the molar ratio of the mixed salt solution concentration, $NH_4HCO_3$ was weighed and dissolved in distilled water at a concentration of 1:4. The mixed salt solution was heated in the electrothermal bath at 55 ℃, and the precipitator solution ($NH_4HCO_3$) was slowly dripped into the mixed salt solution with stirring. The rotor speed was increased, and the water bath temperature was maintained at 55 ℃ for 3 to 4 hours. The precipitate was washed 3 times and centrifuged, and a $Ni_{0.8}Co_{0.1}Mn_{0.1}CO_3$ mixed precipitate was obtained. The precipitate was dried at 120 ℃ in an oven for 12 hours. $LiOH·H_2O$ particles (excess 5%) were mixed and ground for 3 hours at a molar ratio of 1.05:1 (Li: Ni Co Mn) [9]. Finally, the precursor $LiNi_{0.8}Co_{0.1}Mn_{0.1}CO_3$ was sintered in a muffle furnace. The sintering temperature and sintering time were increased due to the lower partial pressure of oxygen in the furnace. The mixed precipitate was put into the crucible and presintered at 500 ℃ for 5 hours and then sintered at 750 ℃ for 15 hours. The heating rate of the muffle furnace was

3 ℃ $min^{-1}$. The target product $LiNi_{0.8}Co_{0.1}Mn_{0.1}O_2$ was obtained after natural cooling. Finally, the $LiNi_{0.8}Co_{0.1}Mn_{0.05}Al_{0.05}O_2$ (811-Al), $LiNi_{0.8}Co_{0.15}Al_{0.05}O_2$ (NCA), $LiNi_{0.7}Co_{0.15}Mn_{0.15}O_2$, $LiNi_{0.7}Co_{0.15}Al_{0.15}O_2$, $LiNi_{0.7}Co_{0.15}Mn_{0.1}Al_{0.05}O_2$ cathode materials were prepared by the same procedure.

### *2.2 Materials Characterization*

The morphology and structure of the sample particles were characterized by X-ray diffraction (XRD) and Cu-$K_\alpha$ as a radiation source (X`Pert PRO, PANalytical) in the range of 10 to 80° [3]. To analyse the morphology and crystal structure of the samples, scanning electron microscopy (SEM-UItra 55) and transmission electron microscopy (TEM-Zeiss Libra 200 FE) were used [10]. Additionally, the super-high-resolution scanning electron microscope (HRTEM-Zeiss Libra 200 FE) can observe the atomic or molecular structure of the material in a three-dimensional stereoscopic form.

### *2.3 Electrochemical Measurements*

First, the 80% active material was uniformly mixed with 10% acetylene black (super P) and 10% polyvinylidene fluoride (PVDF). Second, N-methyl-2-pyrrolidone (NMP) was ground fully and then added to the mixture to prepare the electrode plate. Third, the slurry was evenly dispersed on aluminium foil and dried in the drying box for 12 to 15 hours. Finally, a perforator was used to punch the working battery into the disk. At the same time, a half-cell using a CR2016 coin was assembled in a glove box filled with argon using lithium foil as the electron pair and a polypropylene microporous film (Celgard 2300) as the separator [11]. The commercial battery from the Capchem Company was introduced last. At room temperature, the battery test system was used to charge and discharge the battery at a current rate of 0.1 C. To further measure the rate performance, the current density was increased to 0.2 C, 0.5 C, 1 C and then dropped to 0.1 C (1c=147 $mAhg^{-1}$) [3].

## 3. RESULTS AND DISCUSSION

The crystal structure of the 811 cathode material was studied by X-ray diffraction (XRD). As shown in Fig. 1, all the observed peaks can be indexed to the $LiNi_{0.8}Co_{0.1}Mn_{0.1}O_2$ layered structure with a spatial group of R3m [6]. In addition, there are no other peaks in the XRD diagram; thus, the purity of the 811 cathode material can be determined. The diffraction peak is sharp, and the splitting degree of the (006)/(012), (018)/(110) peak is obvious, which indicates that the material has a good layered structure [12]. In the $LiNi_{0.8}Co_{0.1}Mn_{0.1}O_2$ structure, Li is at the 3a site of the structure, Ni, Co, and Mn are at the 3b site, and O is at the 6c site with its position distorted along the C axis. The structure is the division of the 006/102 peak in the XRD spectrum [13]. Generally, the ratio of $I_{003}$ to $I_{104}$ peak is used to measure the degree of cation mixing in layered structures. If this value is greater than 1.2, the Li-Ni mixed arrangement is low, as seen from the X-ray diffraction image analysis of the

811 batteries. The value of $I_{003}/I_{104}$ is 1.40, which indicates that the 811 prepared by the coprecipitation method has a low degree of mixing and a good layered structure. However, for the 811, 811-Al, NCA, $LiNi_{0.7}Co_{0.15}Mn_{0.15}O_2$, $LiNi_{0.7}Co_{0.15}Al_{0.15}O_2$, and $LiNi_{0.7}Co_{0.15}Mn_{0.1}Al_{0.05}O_2$ samples, the peaks from 37.5° to 40° were detected at 2θ [11]; it is not difficult to see that the (006) and (012) peaks of both the Al- and the Mn-doped materials ($LiNi_{0.8}Co_{0.1}Mn_{0.05}Al_{0.05}O_2$ and $LiNi_{0.7}Co_{0.15}Mn_{0.1}Al_{0.05}O_2$) are not obviously split, which means that the lamellar structure is not well developed [14], and the ratio of $I_{003}/I_{104}$ is less than 1.2.

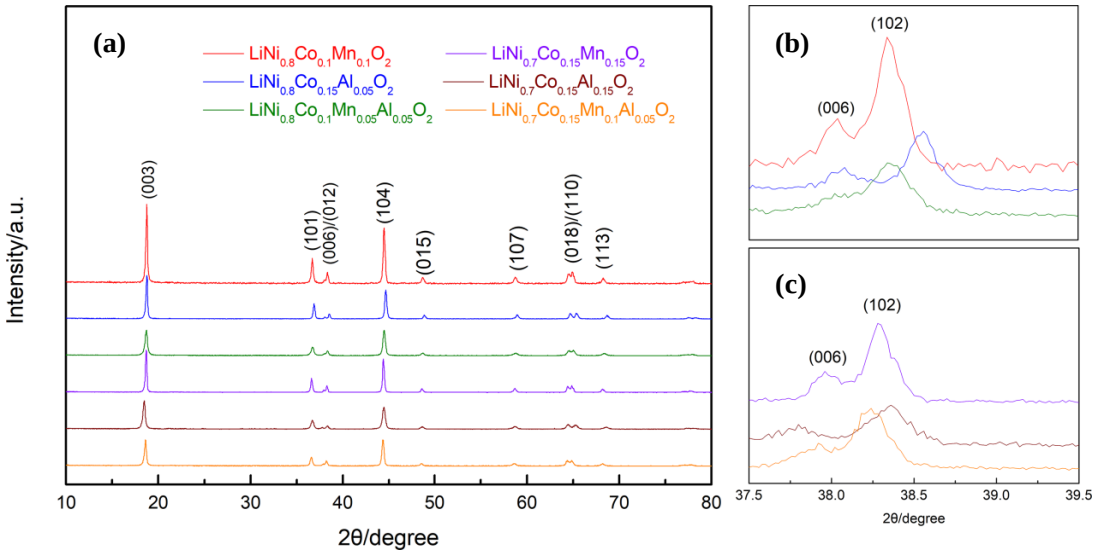


**Figure 1.** X-ray diffraction of 811, NCA, NCA-Mn, $LiNi_{0.7}Co_{0.15}Mn_{0.15}O_2$, $LiNi_{0.7}Co_{0.15}Al_{0.15}O_2$, $LiNi_{0.7}Co_{0.15}Mn_{0.1}Al_{0.05}O_2$.

This may be due to the addition of Mn and Al at the same time, which will drive some of the $Ni^{2+}$ to occupy the positions of the $Li^+$ in the intermediate layer of the crystal structure, while $Li^+$ will enter the position of the transition metal layer, thus forming a mixture of lithium and nickel in the lattice. Therefore, it can be predicted that this will affect the electrical properties of the materials.

Fig. 2 presents the SEM images of 811, 811-Al and NCA, which shows the structure and morphology of the samples. The structure shows that Al/Mn substitutions with 811 as the carrier have a great influence on the surface morphology and the particle size of the materials. From Fig. 2, it can be seen that the surface of sample 811 is smooth, mainly formed by the aggregation of some small grains, and the particle size is approximately 200~350 nm. However, 811-Al and NCA show that the agglomeration phenomenon is more serious than that of 811, and the particle size is also larger, especially the surface of 811-Al, which is coarser than that of NCA. It can be predicted that its electrochemical performance would be worse than that of 811 and NCA. Fig. 3 is the TEM image of 811, which has a grain spacing of 0.47 nm and belongs to the (003) plane of the layered structure [14]. Therefore, there is proof that 811 and 811-Al are both layered structure materials.

In Fig. 4, we show the first charge/discharge curves of all samples at 0.1C. From this figure, we can see that 811, 811-Al and NCA have a flat initial discharge platform, and the charge/discharge

curve is smooth with an initial capacity of 162.8 $mAh \cdot g^{-1}$, 139.7 $mAh \cdot g^{-1}$ and 95.7 $mAh \cdot g^{-1}$, respectively. In contrast, with similar capacities, the initial charge-discharge curves of the low nickel materials $LiNi_{0.7}Co_{0.15}Mn_{0.15}O_2$, $LiNi_{0.7}Co_{0.15}Al_{0.15}O_2$ and $LiNi_{0.7}Co_{0.15}Mn_{0.1}Al_{0.05}O_2$ are inclined with an initial capacity of 120.7 $mAh \cdot g^{-1}$, 102.6 $mAh \cdot g^{-1}$ and 103.9 $mAh \cdot g^{-1}$, respectively, which shows that the 811, 811-Al and NCA materials have a low degree of electrode polarization. According to the charge-discharge capacity of the first cycle (as shown in Fig. 4), we measured the specific capacities (charge specific capacity, Cc and discharge specific capacity, Dc), the remaining capacity after 100 cycles and the capacity retention rate of all samples, as shown in Table 1.

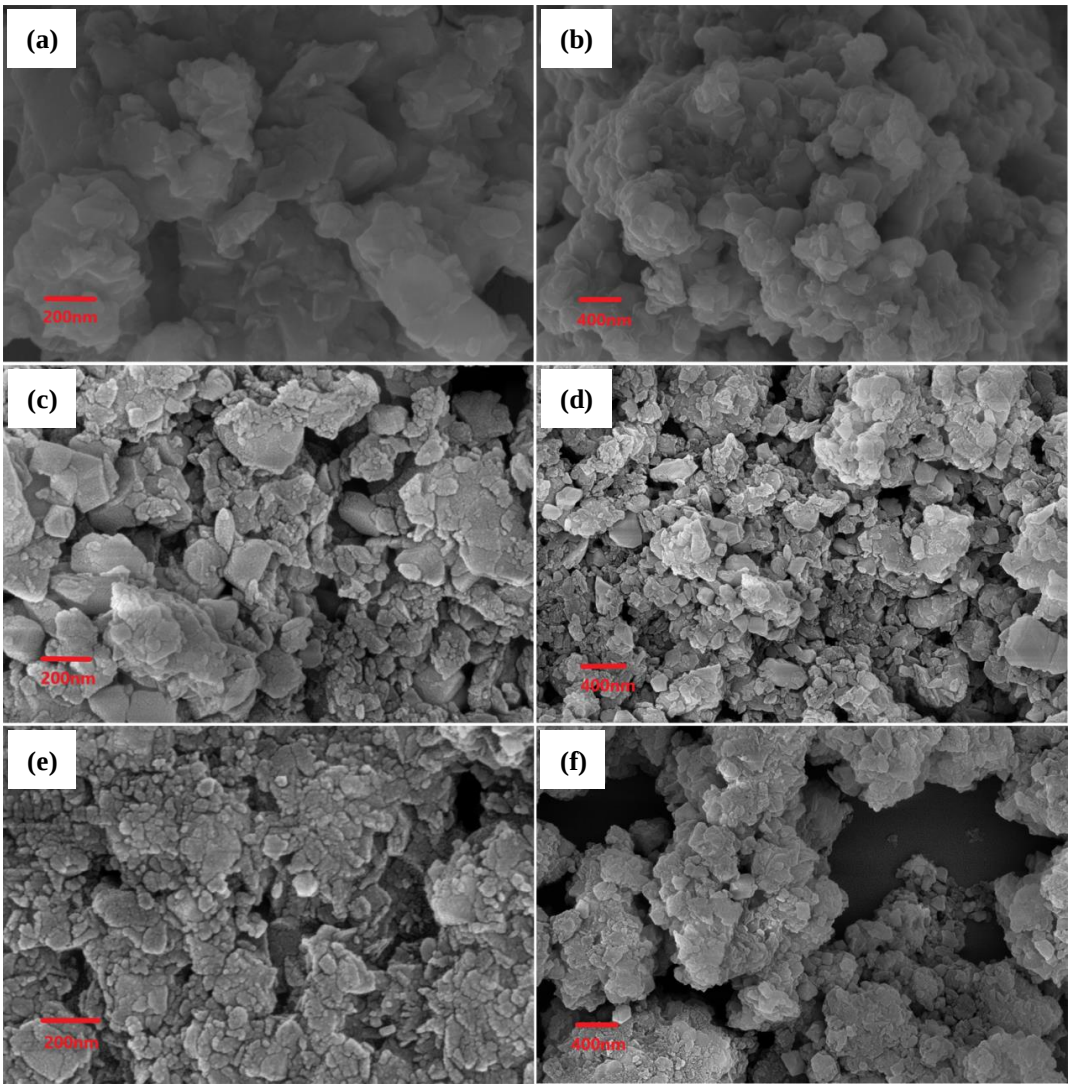


**Figure 2**. SEM image of (a,b) 811, (c,d) NCA and (e,f) 811-Al (or NCA-Mn).

To study the potential effect of Al/Mn substitutions on the cell performance, 811 was used as the carrier, and the constant current density was measured at 0.1 C between 2.5 V and 4.5 V (vs. Li/Li+). The results are shown in Fig. 5. As shown in Fig. 5, the reversible capacity of all the samples was significantly reduced. It is not difficult to see that 811 has a higher capacity and cycle retention rate; after 100 cycles, the battery capacity is 134.6 $mAhg^{-1}$, and the cycle retention rate is 82.7%. After

100 cycles using the $LiNi_{0.7}Co_{0.15}Mn_{0.15}O_2$ material, the battery capacity is 102.4 $mAhg^{-1}$ with a cycle retention rate of 84.5%.

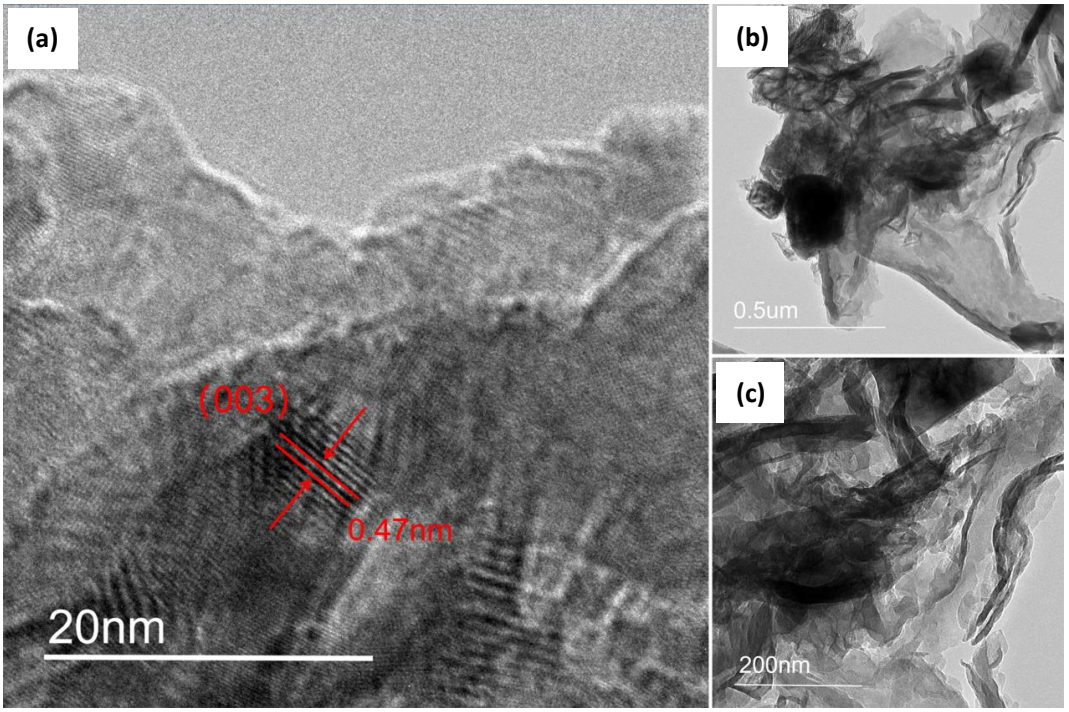


**Figure 3**. TEM images of 811 samples.

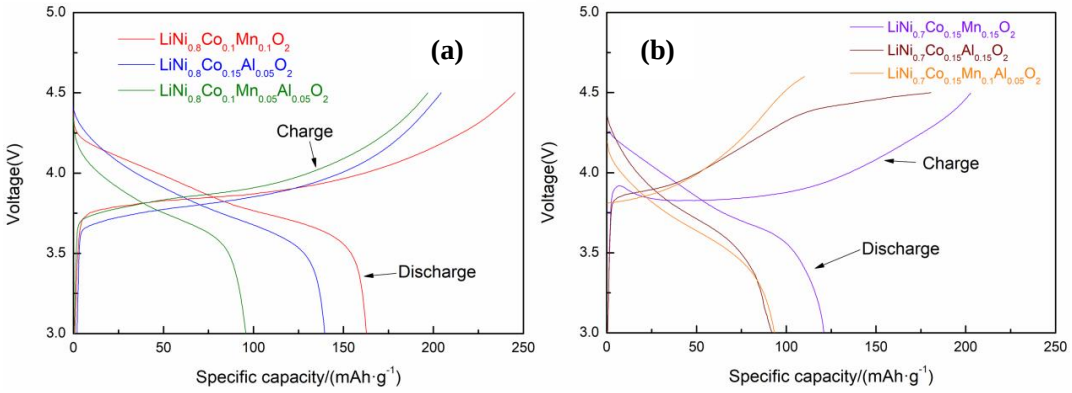


**Figure 4.** The first charge/discharge curve of (a) 811, NCA, 811-Al (or NCA-Mn), and (b) $LiNi_{0.7}Co_{0.15}Mn_{0.15}O_2$, $LiNi_{0.7}Co_{0.15}Al_{0.15}O_2$, $LiNi_{0.7}Co_{0.15}Mn_{0.1}Al_{0.05}O_2$ samples.

Therefore, nickel can significantly increase the battery capacity. However, the stability of the high-nickel material is reduced. Although the stability of 811 is higher than that of $LiNi_{0.7}Co_{0.15}Mn_{0.15}O_2$, the stability is less than that of the low-nickel material. When we compared NCA with $LiNi_{0.7}Co_{0.15}Al_{0.15}O_2$, we found that the performance of $LiNi_{0.7}Co_{0.15}Al_{0.15}O_2$ was poor.

**Table 1.** The specific capacities (charge specific capacity, Cc and discharge specific capacity, Dc) of all samples, the remaining capacity after 100 cycles and the retention ratios.

| Sample | Cc ($mAhg^{-1}$) | Dc ($mAhg^{-1}$) | after 100 times Dc ($mAhg^{-1}$) | retention ratios (%) |
|---|---|---|---|---|
| $LiNi_{0.8}Co_{0.1}Mn_{0.1}O_2$ | 245.2 | 162.8 | 135 | 82.7 |
| $LiNi_{0.8}Co_{0.15}Al_{0.05}O_2$ | 204.3 | 139.7 | 71 | 50.8 |
| $LiNi_{0.8}Co_{0.1}Mn_{0.05}Al_{0.05}O_2$ | 196.9 | 95.7 | 30 | 23.6 |
| $LiNi_{0.7}Co_{0.15}Mn_{0.15}O_2$ | 187 | 121 | 102.4 | 84.5 |
| $LiNi_{0.7}Co_{0.15}Al_{0.15}O_2$ | 180.6 | 102.6 | 27.3 | 25.9 |
| $LiNi_{0.7}Co_{0.15}Mn_{0.1}Al_{0.05}O_2$ | 110.2 | 103.9 | 23.5 | 22.7 |

After 100 cycles of charge and discharge, the cycle retention rate of NCA was 50.8%. The cycle retention rate of $LiNi_{0.7}Co_{0.15}Al_{0.15}O_2$ was only 25.9%. Due to the similar structure and particle size between 811-Al and NCA, the battery performance of 811-Al is much lower than that of 811, which is also 100 cycles. The capacity of 811-Al is 23.6 $mAhg^{-1}$, and the retention rate is 22.7%.

This phenomenon is considered to be related to the following reasons:

(i) The effect of Li-Ni exchange (cation mixing) [15]. Liang's article mentioned that Mn has a better stabilization effect on layered materials; the main effect is to improve the structure stability of layered oxides [16]. At the same time, it can inhibit the precipitation of oxygen, thus inhibiting the disorder of cations [17-18]. Li-Ni exchange often results in a loss of material properties and capacity. Because the $Li^+$ ion radius (0.076 nm) is similar to the $Ni^{2+}$ ion radius (0.069 nm), $Ni^{2+}$ often exists in the Li layer [19-20]. As shown in Fig. 1, replacing Mn with Al can reduce the exchange effect of Li-Ni because Al cannot interfere with the layered structure [21-22]; this substitution will also reduce the performance and stability in the charge/discharge reaction. In the experiment, we measured the $I_{003}$ to $I_{104}$ ratio of NCA, which was equal to 1.5; thus, we can prove that this conclusion is correct. However, when we partially replace Mn with Al, we find that the mixed discharge of Li-Ni is more serious. We think that the addition of Al breaks the delicate balance of the 1:1 molar ratio between Co and Mn and aggravates the exchange of Li-Ni. This seriously affects the performance and cycle stability of the battery.

(ii) The effect of the change in valence state on the experimental results of Ni during calcination. In the preparation of cathode materials 811, NCA, and NCA-Mn, we chose to use the Mafer furnace to calcinate the precursor of the above materials due to the influence of laboratory equipment. The effect is that the partial pressure of oxygen is insufficient, which results in the incomplete oxidation of $Ni^{2+}$ to $Ni^{3+}$. The existence of more $Ni^{2+}$ in the lattice hinders the delamination of $Li^+$ between layers, and the collapse of the layered structure is caused by the release of $Li^+$ between layers. Therefore, the charge and discharge capacity of the ternary positive batteries we fabricated is generally low.

(iii) The effect of ion valence variation on the mixed discharge of Li-Ni during the charge-discharge process. In the 811 cathode material battery, the average valence of Ni/Co/Mn is +3. During the charging of the lithium-ion battery, Li "detaches" from $LiNi_{0.8}Co_{0.1}Mn_{0.1}O_2$ (811) and releases an electron; the $Li^+$ migrates to the graphite surface of the negative electrode through the diaphragm and electrolyte and then inserts into the graphite structure. To ensure the conservation of electrical charge, the average valence of Ni/Co/Mn will rise, and the average valence state will be +4. When the discharge begins, electrons run from the negative pole through the electron conductor back to the positive pole. $Li^+$ jumps back from the negative pole into the electrolyte; "climbs" into the small hole in the diaphragm, embeds into the positive pole, and at the same time combines with the running electrons to complete the discharge process. In this process, we believe that the capacity of NCA is lower than that of the material 811 because $Li^+$ will cause a change in the Ni/Co/Mn ion valence state during the process of deintercalation. When charging, $Al^{3+}$ has good stability; in order to ensure the balance of the valence state, it causes more Ni/Co valence states to rise. The effect is that more $Ni^{4+}$ reduces to $Ni^{2+}$ and mixes with $Li^+$ to form a Li-Ni mixed arrangement, which reduces the capacity of the system. From Fig. 1, we can directly see that the Li-Ni mixing of NCA-Mn material and $Li_{0.7}Co_{0.15}Mn_{0.1}Al_{0.05}O_2$ material is very serious; the ratio of (003)/(104) of NCA-Mn is 1.02, and the ratio of (003)/(104) of $LiNi_{0.7}Co_{0.15}Mn_{0.1}Al_{0.05}O_2$ is 1.01. The serious mixing of Li and Ni directly affects the capacity and cycle performance of the battery, as shown in Fig. 5.

We tested the charge-discharge rate of the battery, as shown in Fig. 6. Under the different current rates of 0.1 C to 1 C, the rate performance of the battery was tested 10 times, and the test results are shown in Fig. 5. As shown in Fig. 5, although the charge-discharge capacity of NCA is less than that of 811, the rate performance of NCA is better.

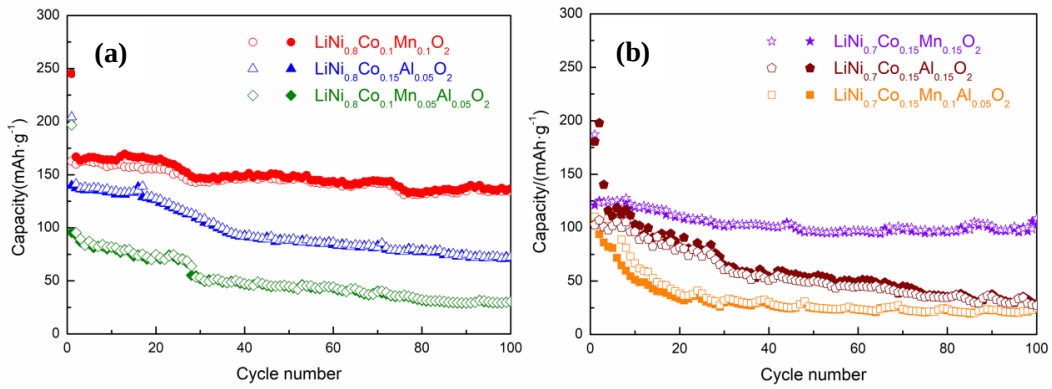


**Figure 5.** The cycling performance of (a) 811, NCA, 811-Al (or NCA-Mn), and (b) $LiNi_{0.7}Co_{0.15}Mn_{0.15}O_2$, $LiNi_{0.7}Co_{0.15}Al_{0.15}O_2$, $LiNi_{0.7}Co_{0.15}Mn_{0.1}Al_{0.05}O_2$ samples.

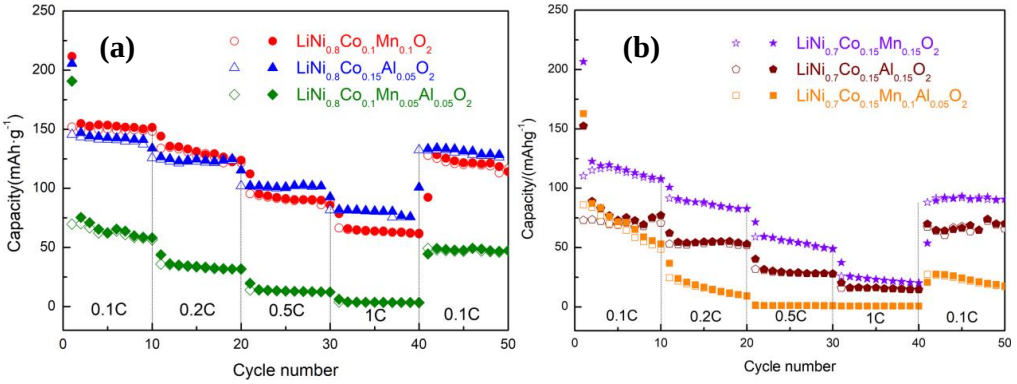


**Figure 6.** Charge-discharge capacity and discharge rate capacity of (a) 811, NCA, 811-Al (or NCA-Mn), and (b) $LiNi_{0.7}Co_{0.15}Mn_{0.15}O_2$, $LiNi_{0.7}Co_{0.15}Al_{0.15}O_2$, $LiNi_{0.7}Co_{0.15}Mn_{0.1}Al_{0.05}O_2$ samples.

Therefore, we can judge that $Al^{3+}$ plays an important role in improving the rate performance of batteries. With the occurrence of this phenomenon, we think that Al can effectively inhibit the formation of oxygen vacancies [19], and the formation of oxygen vacancies can promote the formation of cationic disorders. Thus, the rate performance of the battery is improved.

## 4. CONCLUSIONS

In this experiment, the effects of the coprecipitation method on the cycle and performance of lithium-ion battery material $LiNi_{0.8}Co_{0.1}Mn_{0.1}O_2$ and other elements were studied. We find that $LiNi_{0.8}Co_{0.1}Mn_{0.1}O_2$ has good cyclic and cyclic characteristics, and the excellent performance is due to the role of Mn. Because of the existence of Mn, the mixing effect of Li-Ni is suppressed, and the deintercalation of Li is reduced. The capacity and cycle performance of the battery are improved. Therefore, a reasonable conclusion of this experiment is that the Mn/Al substitution modification, with 811 as the carrier, proves that 811 have good application prospects.

## References

1. G. Qin, X. Wu, J. Wen, J. Li, M. Zeng, *ChemElectroChem*, 6 (2019) 911.
2. G. Qin, M. Zeng, X. Wu, J.Wen, J. Li, *J. Mater. Sci-Mater. El.*, 29 (15) (2018) 12944.
3. Y. Mu, M. Zeng, X. Wu, X. Tong, *Int. J. Electrochem. Sci.*, 12 (2017) 6045.
4. Y.X. Qian, Y.F. Deng, L.N. Wan, H.J. Xu, X.S. Qin, G.H. Chen, *J. Phys. Chem. C*, 118 (2014) 15581.
5. L.B. Song, F.L. Tang, Z.L. Xiao, Z. Cao, H.L. Zhu, A.X. Li, *J. Electron. Mater.*, 47 (2018) 5896.
6. A. Iqbal, L. Chen, Y. Chen, Y.X. Gao, F. Chen, D.C. Li, *Int. J. Min. Met. Mater.*, 25 (2018) 1473.
7. X. Wu, M. Zeng, L.G. Wang, J. Li, *J. Alloy. Compd.*, 780 (2019) 897.
8. G.B. Zhong, Y.Y. Wang, X.J. Zhao, *J. Power Sources*, 216 (2012) 368.
9. W. Li, X. Liu, H. Celio, P. Smith, A. Dolocan, M.F. Chi, A. Manthiram, *Adv. Energy Materi.*, 8 (2018) 1703154.

10. Y.D. Xu, W. Xiang, Z.G. Wu, C.L. Xu, Y.C. Li, X.D. Guo, B.H. Zhong, *Electrochim. Acta*, 268 (2018) 358.
11. X. Tong, M. Zeng, J. Li, H. Xu, M.L. Du, F.Y. Li, *Int. J. Electrochem. Sci*., 11 (2016) 7333.
12. J. Zheng, P. Yan, L. Estevez, C.M. Wang, J.G. Zhang, *Nano energy*, 49 (2018) 538.
13. G. Li, L. Qi, P. Xiao, Y.L. Yu, X. Chen, W.S. Yang, *Electrochim. Acta*, 270 (2018) 319.
14. F. Wu, Q. Li, L. Chen, Y. Lu, Y.F. Su, L.Y. Bao, R.J. Chen, S. Chen, *ChemSusChem*, 12 (2019) 935 .
15. C. Liang, F. Kong, R.C. Longo, C.X. Zhang, Y.F. Nie, Y.P. Zheng, K. Cho, *J. Mater. Chem. A*, 5 (2017) 25303.
16. J. Zheng, W.H. Kan, A. Manthiram, *ACS appl. Mater. Inter.*, 7(2015) 6926.
17. A.Manthiram, J.C.Knight, S.T. Myung, S.M. Oh, Y.K. Sun, *Adv. Energy Mater.*, 6 (2016) 1501010.
18. H.W. Tang, Z.H. Zhu, Z.R. Chang, Z.J. Chen, X.Z. Yuan, H. Wang, *Electrochem. Solid St.*, 11 (2008) 34.
19. K.Min, S.W. Seo, Y.Y. Song, H.S. Lee, E. Cho, *Phys. Chem. Chem. Phys.*, 19 (2017) 1762.
20. W. Liu, P. Oh, X. Liu, M.J. Lee, W. Cho, S. Chae, Y. Kim, J. Cho, *Angew. Chem. Int. Edit.*, 54 (2015) 4440.
21. R. Stoyanova, E. Zhecheva, E. Kuzmanova, *Solid State Ionics*, 128 (2000) 1.
22. Y. Nishida, K. Nakane, T. Satoh, *J. Power Sources*, 68 (1997) 561.
23. W.M. Liu, M.L. Qin, C.W. Gao, D.H. Yu, Y.Z. Yue, Green and low-cost synthesis of $LiNi_{0.8}Co_{0.15}Al_{0.05}O_2$ cathode material for Li-ion batteries. *Mater. Lett*., 246 (2019) 153.